Encoded-Fusion-Based Quantum Computation for High Thresholds with Linear Optics

Wooyeong Song,[1] Nuri Kang,[1,2] Yong-Su Kim,[1,3] and Seung-Woo Lee[1,*]
[1]Center for Quantum Information, Korea Institute of Science and Technology (KIST), Seoul 02792, Republic of Korea
[2]Department of Physics, Korea University, Seoul 02841, Republic of Korea
[3]Division of Nano and Information Technology, KIST School, Korea University of Science and Technology, Seoul 02792, Republic of Korea

(Received 11 November 2023; accepted 17 May 2024; published 1 August 2024)

We propose a fault-tolerant quantum computation scheme in a measurement-based manner with finite-sized entangled resource states and encoded-fusion scheme with linear optics. The encoded fusion is an entangled measurement devised to enhance the fusion success probability in the presence of losses and errors based on a quantum error-correcting code. We apply an encoded-fusion scheme, which can be performed with linear optics and active feedforwards to implement the generalized Shor code, to construct a fault-tolerant network configuration in a three-dimensional Raussendorf-Harrington-Goyal lattice based on the surface code. Numerical simulations show that our scheme allows us to achieve up to 10 times higher loss thresholds than nonencoded fusion approaches with limited numbers of photons used in fusion. Our scheme paves an efficient route toward fault-tolerant quantum computing with finite-sized entangled resource states and linear optics.

DOI: 10.1103/PhysRevLett.133.050605

Toward scalable quantum computation [1–5], photonic systems have been considered as leading platforms thanks to high-quality sources and detectors, efficient modularity and connectivity, and long decoherence time at room temperature [6–8]. Especially, extremely fast measurements on photons make them suited for measurement-based quantum computing [9–13]. In measurement-based quantum computing, universal gate operations are realizable via single-qubit measurements applied on entangled resource states prepared off-line. However, due to the nondeterministic fusion [14,15]—a projective measurement on entangled photons—and loss in photonic platforms, an extensive number of entangled photons are consumed to prepare the resource states for fault-tolerant architectures [9–13].

To circumvent such formidable prerequisites, fusion-based quantum computing (FBQC) was recently proposed [16–18], performed via fusions between constant-sized resource states without extensive entanglement prepared and with stability maintained during the process. Its architecture consists of resource states and fusions, which are connected to each other to create a specific network configuration called a fusion network. By constructing a fusion network, a quantum error-correcting (QEC) code can be implemented. For example, surface code is implemented as three-dimensional Raussendorf-Harrington-Goyal (RHG) lattice [2–5]. The details of FBQC are in Ref. [16]. The fusion thus plays a crucial role in FBQC and its efficiency directly affects the computation performance. However, the fusion success probability is limited by 50% with linear optics. Moreover, its boost with ancillary entangled photons [19] turned out to be in a trade-off with the loss tolerance [16]. Therefore, fusions in the presence of loss degrade the performance of FBQC significantly, which becomes more crucial when the system size increases, and, as a result, it may be still challenging to build a fault-tolerant architecture in photonic quantum computing platforms.

In this Letter, we propose a scheme for fault-tolerant quantum computation with finite-sized entangled states and fusions protected by QEC. An *encoded fusion* is devised to enhance the fusion success probability under loss by QEC. We apply an encoded fusion designed based on (n, m)-generalized Shor [20] or parity code [21–23], implementable with linear optics and active feedforwards, to construct a RHG lattice. Numerical simulations show that our scheme achieves up to 10 times higher loss thresholds for individual photons than nonencoded fusion approaches [16–18] with a limited number of photons used per fusion. Specifically, a record-high threshold 14% is achieved with moderate encoding numbers, e.g., (7,4) with single-step feedforward. We also show that when adopting the same encoded resource states, our scheme can reach significantly higher loss thresholds than FBQC [16] by consuming fewer photons.

Our approach, while motivated from Ref. [16], offers a different way toward fault tolerance. The result demonstrates that a concatenation of two QECs, one for the fusion and the other for the network configuration, can dramatically enhance the loss thresholds. A similar approach has been recently introduced in Ref. [24]. We here focus on RHG lattice and resource states used in Ref. [16] for direct

*Contact author: swleego@gmail.com

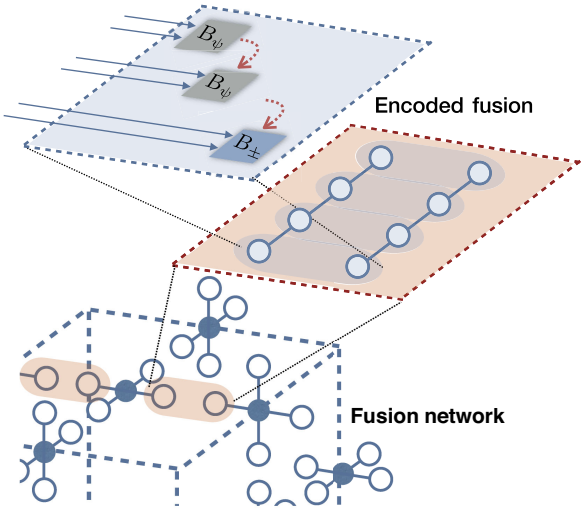

FIG. 1. Schematics of EFBQC. In a fusion network, the photons participating in fusions are encoded in a QEC code, and an encoded-fusion protocol is performed actively in a concatenative manner between encoded qubits.

comparison, but our scheme is not limited to a specific configuration but generally applicable for various architectures and resource states [17,18].

Encoded-fusion-based quantum computation—Let us introduce the encoded-fusion-based quantum computing (EFBQC). In EFBQC, the process to create a fusion network and logical gate operations is conceptually equivalent to FBQC [16] except that fusions are replaced with encoded fusions. Compared to FBQC, however, EFBQC is aimed more at correcting the errors from resource states, fusion failure, and photon loss by fusion itself, while constructing a fusion network, as illustrated in Fig. 1. Fusions are applied between resource states to construct a specific fusion network. A fusion network can thus be designed appropriately such that all measurements are projections onto stabilizer states, and corresponding QEC schemes based on the stabilizer formalism can then be applied to achieve the fault tolerance. We here focus on fusion networks in which fusions are the projection onto a particular stabilizer basis, i.e., the Bell basis. Such a fusion, called Bell fusion, can be described as X_1X_2 and Z_1Z_2 measurements on two qubits 1 and 2, whose operators form a stabilizer group $\langle X_1X_2, Z_1Z_2\rangle$. The outcomes of all Bell fusions combine to perform parity checks to enable error correction, e.g., by surface code.

To realize FBQC with linear optics, we should account for two imperfections leading to erasures of measurement outcomes: (i) photon loss, a dominant error source in any photonic platforms, and (ii) the 50% limit of the success probability of Bell fusion or equivalently Bell-state measurement (BSM) with linear optics. Specifically, a fusion failure can be treated as an erasure of either X_1X_2 or Z_1Z_2 outcome. Any loss in each fusion causes a complete erasure of outcomes. As a result, such erasures reduce the error tolerance of FBQC significantly, which becomes a crucial factor in building a linear optical scalable architecture. It turned out that boosting the success probability with ancillary entangled photons [19] increases the rate of erasures and eventually harms the loss tolerance of FBQC [16].

On the other hand, in EFBQC, encoded fusions play a role logically as X_1X_2 and Z_1Z_2 on two encoded qubits 1 and 2 of loss so that all events of erasures of X_1X_2 and Z_1Z_2 can be suppressed. Therefore, all fusion outcomes are consistent with the resource state stabilizers, and, in principle, error correction in fusion network exhibits the maximum performance of the fault tolerance (see Supplemental Material for details [25]). An encoded fusion can be implemented by performing multiple linear-optic BSMs consecutively with a QEC protocol that enables increasing the success probability even in the presence of photon loss, as we introduce in the following.

Encoded fusion with linear optics—Several schemes have been proposed to overcome the 50% limit of the fusion success probability with linear optics by using ancillary entangled photons [19,30], squeezing [31], and Greenberger-Horne-Zeilinger (GHZ) encoding [32,33]. However, employing a large number of photons in fusion generally is at a higher risk of photon loss, which offsets an advantage and eventually is in a trade-off with the loss threshold of FBQC [16]. In contrast, an encoding only against photon loss does not solve the problem induced by the low efficiency of fusion. Therefore, it is essential to enhance the success probability of fusion while suppressing the effects of photon loss that may occur in the fusion and resource state preparation.

We introduce a method to enhance both the fusion success probability and loss tolerance by a QEC protocol with linear optics. Consider the (n, m)-Shor or parity code [21] with dual-rail qubits as a representative example. We define the logical basis as $|0_L\rangle = |+^{(m)}\rangle^{\otimes n}$ and $|1_L\rangle = |-^{(m)}\rangle^{\otimes n}$, where $|\pm^{(m)}\rangle = (|H\rangle^{\otimes m} \pm |V\rangle^{\otimes m})/\sqrt{2}$ consists of n blocks, each of which includes m photons in $|\pm\rangle$ state. Interestingly, the encoded Bell states $|\Psi^\pm\rangle = |0_L\rangle|1_L\rangle \pm |1_L\rangle|0_L\rangle$ and $|\Phi^\pm\rangle = |0_L\rangle|0_L\rangle \pm |1_L\rangle|1_L\rangle$ can be decomposed into n number of block-level Bell states, each of which in turn is decomposed into m number of photonic Bell states [25]. While a linear-optic BSM can discriminate only two out of the four Bell states, such characteristics of the encoded states make it possible to logically distinguish the Bell states by a series of $n \times m$ linear-optic BSMs with much higher efficiencies.

We now sketch the encoded-fusion protocol based on linear optics and active feedforwards (details in Supplemental Material [25]).

In physical qubit level, we use three types of linear-optic BSMs discriminating $|\psi^+\rangle/|\psi^-\rangle$, $|\psi^+\rangle/|\phi^+\rangle$, and $|\psi^-\rangle/|\phi^-\rangle$ deterministically, denoted as B_ψ, B_+ and B_-, respectively. Note that BSM can be implemented by basic

linear-optical elements such as polarizing beam splitters, wave plates, and photon detectors, which can discriminate only two out of the four Bell states. The type can be easily changed by simply rotating wave plates on the inputs of polarizing beam splitters. The protocol is as follows: (i) In each block, B_ψ is applied on each pair of photons randomly selected from distinct encoded qubits. Repeat until B_ψ succeeds, detects a loss, or consecutively fails $j \leq m-1$ times (a predetermined optimized number). (ii) B_+ or B_- is applied on the remaining photon pairs, if any B_ψ succeeded with the result $|\psi^+\rangle$ and $|\psi^-\rangle$, respectively. For loss detection and j-times failure, B_+ or B_- is randomly selected. (iii) Total n times of block-level protocols, (i) and (ii), are performed independently.

In each block, the sign $(\pm)$ is identified by any success of B_ψ, and the letter (ψ, ϕ) is also identified based on the results of all $B_\pm$ performed on remaining photon pairs. So, full discrimination is possible unless loss occurs, and at least the sign can be identified with any single success of B_ψ or $B_\pm$. We denote the full discrimination and failure probability as p_s and p_f, respectively. The probability of only sign discrimination is then $1-p_f-p_s$.

By collecting all the results of independently performed n-times block-level protocols, the logical result is determined. The letter is the same with any determined block-level result. The sign can be identified by counting the number of minus $(-)$ signs from block-level results. As a result, the success probability of encoded fusion based on (n,m)-Shor code is obtained as $P_s(\eta) = (1-p_f)^n - (1-p_s-p_f)^n$ with a given loss rate η per photon, which becomes $1-2^{-mn}$ when no loss occurs. Note that, in contrast to the boost scheme with ancillary entangled photons [19], the encoded fusion can succeed with arbitrarily high rates with a moderate encoding number (n,m) in the presence of photon loss [25].

Encoded-fusion networks and resource states—A fusion network is constructed to implement a foliated QEC code [34]. A standard approach implementing the surface code leads to form a three-dimensional RHG lattice [2–5]. A variation of surface code for biased noises, i.e., $XZZX$ code [35,36], can be implemented by constructing a $XZZX$ lattice fusion network [17]. The aforementioned lattice models were shown to be fabricated by employing 4-star and 6-ring shape resource states introduced in Ref. [16]. Linear cluster states can also be used as resource states [18] to create a foliated Floquet color code architecture [37,38]. We here focus on RHG lattice structures for the direct comparison with FBQC [16].

The process to form a RHG lattice and the corresponding resource states are logically equivalent to FBQC. The encoded-fusion networks in RHG lattice can thus be constructed by applying encoded fusions on the encoded 4-star or 6-ring resource states as illustrated in Fig. 2. However, not only the resource states but also the fusion schemes are here reformulated as encoded forms, e.g., by

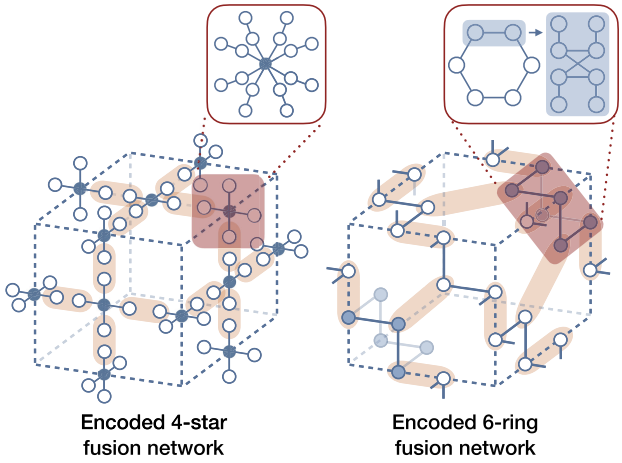

FIG. 2. For the direct comparison with FBQC [16], we apply our scheme to the networks in RHG lattice fabricated with the encoded 4-star and encoded 6-ring resource states. The insets illustrate the simplest example with $(n,m)=(2,2)$. The structure and encoded resource states are the same with FBQC [16], while the fusions are replaced with the encoded fusions in orange ovals.

(n,m)-Shor code in the current model. The encoded 4-star and 6-ring resource states have the forms obtained by replacing all the qubits participating in fusion with encoded qubits. As simplest examples, (2,2) encoded 4-star and 6-ring resource states are illustrated in the inset of Fig. 2. Such encoded resource states in arbitrary encoding numbers can be generated straightforwardly by fusing entangled resource states such as GHZ states [9]. For example, the encoded 4-star resource state based on (n,m)-Shor code is composed of $4\times(n\times m)$ photonic qubits, and can be generated by fusing $4n$-GHZ state and $4\times n$ number of $(m+1)$-GHZ states. The generation schemes of encoded resource states are elaborated in Supplemental Material [25]. Note that arbitrary n-GHZ states can be built from 3-GHZ states that are readily available in current photonic technologies [39–46]. Once the resource states are prepared with an encoding number (n,m), the encoded fusions with the same (n,m) are correspondingly applied.

Thresholds of encoded-fusion networks—The performance of fusion networks can be analyzed with two error models: (i) hardware-agnostic error model with the erasure rate P_{erasure} and the measurement (flipped) error rate P_{error}, and (ii) linear-optical error model with the fusion success rate $P_s(\eta)$ and the loss rate η for individual photons. The thresholds of FBQC was analyzed in Ref. [16], in which the correctable regions of two parameters P_{erasure} and P_{error} were evaluated by Monte Carlo simulation, e.g., yielding P_{erasure} thresholds 6.90% for 4-star and 11.98% for 6-ring fusion networks when no measurement error occurs. Photon loss thresholds under the linear-optical error model were then estimated as about 0.25% and 0.78% per individual photon for 4-star and 6-ring fusion networks, respectively [16], assuming boosted fusion success probabilities with ancillary entangled photons [19]. It was also

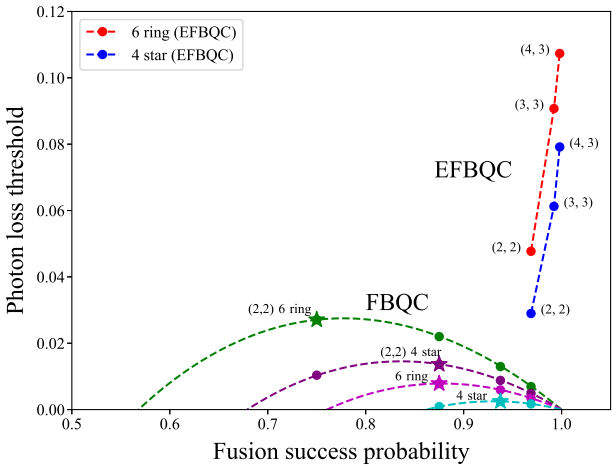

FIG. 3. Photon loss thresholds for different fusion success probabilities $P_s(\eta)$. The green, purple, magenta, and cyan curves show the results of FBQC in Ref. [16]: the dots on the curves represent the cases when the fusion success probability is boosted with different numbers of additional entangled photons, e.g., $P_s(\eta) = 0.75$ with additional 2 photons per physical fusion (additional $2 \times 4 = 8$) for (2,2), and the star shows the maximum value among them. The blue and red dots represent the loss thresholds of EFBQC with different $(n, m) = (2, 2), (3, 3), (4, 3)$ based on encoded 4-star and 6-ring fusion networks, respectively.

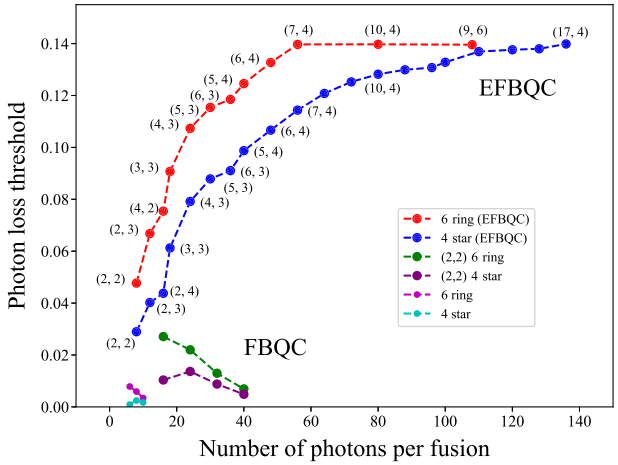

FIG. 4. Photon loss thresholds for the total number of photons used per fusion. The thresholds of EFBQC are maximized by optimizing the encoded-fusion protocol for a given encoding number (n, m). The threshold for EFBQC generally gets higher when increasing the number of photons used per fusion, while the threshold for FBQC boosted with ancillary entangled photons decreases. EFBQCs for encoded 4-star and 6-ring resource states, respectively, yield 11.44% and 13.97% when $(n, m) = (7, 4)$, and both arbitrarily reach up to 14% as increasing (n, m).

shown that FBQC using encoded qubits in (2,2)-Shor code with boosting can achieve a higher threshold, e.g., 2.7% for 6-ring fusion network [16].

Let us now examine the loss thresholds of EFBQC. We employ the same hardware-agnostic model for the direct comparison with FBQC, resulting in the same correctable regions of P_{erasure} and P_{error}. We can then estimate the loss thresholds of encoded-fusion networks based on the linear-optical error model characterized by $P_s(\eta)$ and η by evaluating P_{erasure} and P_{error}. We plot the thresholds of EFBQC against the fusion success probability in Fig. 3 and by changing the total number of photons used per fusion in Fig. 4 with different fusion encoding numbers (n, m). For comparison, we also plot the thresholds of FBQC obtained in Ref. [16].

Figure 3 shows that EFBQC yields much higher loss thresholds and fusion success probabilities than FBQC. The thresholds of FBQC are maximized under a limited fusion success probability and any further boosting degrades these [16]. This implies that additional use of photons increases the risk of loss in FBQC so that the fusion success probability is in a trade-off with the threshold. On the other hand, in EFBQC, the loss thresholds can be improved together with the fusion success probability. Our results show that the proposed encoded-fusion scheme can enhance the success probability by increasing the encoding number (n, m) while suppressing the effect of loss simultaneously, so that the loss thresholds of EFBQC can be dramatically improved. A loss threshold 4.8% per photon is achieved with (2,2) encoded 6-ring resource states in EFBQC, which is almost doubled from 2.7% obtained with the same resource states and additional entangled photons for boosting in FBQC [16], notably by consuming fewer photons and adding only a two-step linear-optical process ($j = 1$). See Supplemental Material for the comparison of resource overheads [25].

In Fig. 4, we plot the loss thresholds of EFBQC numerically maximized in our protocol for given (n, m), and compare the results with FBQC by changing the total number of photons used per fusion. See Supplemental Material for the optimized protocol [25]. It exhibits that, with a fixed number of photons in fusion, EFBQC can achieve much higher thresholds than FBQC. Remarkably, the attained loss thresholds of EFBQC are about 10 times higher than non-encoded and about 5 times higher than encoded FBQCs that were estimated in previous works [16–18]. Specifically, EFBQCs with (7,4) encoded 4-star and 6-ring fusion networks, respectively, reach 11.44% and 13.97% loss thresholds per photon. This implies that a moderate number of additional photons used in fusion can substantially enhance the loss thresholds by our scheme. Note that both 4-star and 6-ring encoded-fusion networks can reach arbitrarily up to 14% by increasing the encoding number (n, m). Such a maximum threshold may be the characteristic of current choices of concatenated QEC codes, i.e., generalized Shor and surface code, and thus possibly can be enhanced further with other codes [17,18].

Remarks—We have proposed a fault-tolerant quantum computation scheme performed in a measurement-based

manner with finite-sized entangled resource states and encoded fusions. In contrast to FBQC schemes [16–18], two different QECs, one for the fusion and the other for the network configuration, are used concatenatively in EFBQC. The encoded fusion is devised to correct photon loss, fusion failure, and resource errors within the fusion process by implementing a QEC code. Moreover, an encoded fusion with (n, m)-Shor code is shown to be efficiently implementable with linear optics and active feedforwards only. We have applied the encoded fusion to construct a fusion network in RHG lattice. By numerical simulations, we have demonstrated that our scheme improves the loss thresholds up to 10 times higher than nonencoded fusion approaches [16–18], and allows us to attain ∼14% loss thresholds per individual photon, which is to our knowledge a record-high threshold among recent achievements in photonic quantum computing platforms [16–18,47]. We have also shown that EFBQC outperforms FBQC with respect to the attainable thresholds by consuming the same number of photons.

We found that Bell *et al.* [24] have similarly studied encoding for fusion to improve thresholds over FBQC [16]; 10.5% is achieved by encoding into a 10-qubit graph code with an adaptive protocol, which is comparable to our results with (4,3) encoded (12-qubit) case, being lower, and higher than (3,3) encoded (9-qubit) case, while our scheme enhances the threshold further up to 14% by increasing the encoding size. Such an optimal graph state can be searched by an exhaustive search method priorly for a given encoding size [24], while applying our scheme for arbitrary high (n, m) is straightforward with the same protocol. Despite being developed independently using different codes and protocols, both schemes provide a common alternative way toward fault tolerance to overcome the limit of standard FBQC. See also Ref. [48] in which high thresholds have been achieved using GHZ-state measurements.

Our scheme can be implemented by linear optics with few-step feedforwards, which is efficiently realizable within current technologies [49,50]. By simply adding one more step of linear-optical process ($j = 1$), EFBQC almost doubles the threshold of (2,2)-Shor code encoded 6-ring network estimated in FBQC [16]. Moreover, numerical optimization shows that only one or two additional steps with a moderate number of photons in encoding, e.g., (7,4) with single-step feedforward ($j = 1$), can yield loss thresholds up to 14% [25]. All required encoded resource states are producible with available entangled photon sources [39–46]. Our scheme is thus readily implementable within current and near-term photonic platforms.

Finally, we note that our approach is not limited to any specific configuration or code, and generally applicable for various architectures by e.g., *XZZX* surface [17] and Floquet color code [18], and resource states, e.g., linear cluster states [18]. Developing encoded-fusion protocols with other QECs [24,51] would be also valuable as next step of research.

Acknowledgments—This research was funded by Korea Institute of Science and Technology (2E32941) and National Research Foundation of Korea (2022M3K4A1094774).

[1] P. Shor, Fault-tolerant quantum computation, in *Proceedings of the 37th Conference on Foundations of Computer Science* (IEEE, New York, 1996), pp. 56–65.
[2] A. G. Fowler and K. Goyal, Topological cluster state quantum computing, Quantum Inf. Comput. **9**, 721 (2009).
[3] A. G. Fowler, M. Mariantoni, J. M. Martinis, and A. N. Cleland, Surface codes: Towards practical large-scale quantum computation, Phys. Rev. A **86**, 032324 (2012).
[4] R. Raussendorf, J. Harrington, and K. Goyal, A fault-tolerant one-way quantum computer, Ann. Phys. (Amsterdam) **321**, 2242 (2006).
[5] R. Raussendorf and J. Harrington, Fault-tolerant quantum computation with high threshold in two dimensions, Phys. Rev. Lett. **98**, 190504 (2007).
[6] S. Slussarenko and G. J. Pryde, Photonic quantum information processing: A concise review, Appl. Phys. Rev. **6**, 041303 (2019).
[7] S. Takeda and A. Furusawa, Toward large-scale fault-tolerant universal photonic quantum computing, APL Photonics **4**, 060902 (2019).
[8] D. E. Browne and T. Rudolph, Resource-efficient linear optical quantum computation, Phys. Rev. Lett. **95**, 010501 (2005).
[9] M. Gimeno-Segovia, P. Shadbolt, D. E. Browne, and T. Rudolph, From three-photon Greenberger-Horne-Zeilinger states to ballistic universal quantum computation, Phys. Rev. Lett. **115**, 020502 (2015).
[10] Y. Li, P. C. Humphreys, G. J. Mendoza, and S. C. Benjamin, Resource costs for fault-tolerant linear optical quantum computing, Phys. Rev. X **5**, 041007 (2015).
[11] D. Herr, A. Paler, S. J. Devitt, and F. Nori, A local and scalable lattice renormalization method for ballistic quantum computation, npj Quantum Inf. **4**, 27 (2018).
[12] J. M. Auger, H. Anwar, M. Gimeno-Segovia, T. M. Stace, and D. E. Browne, Fault-tolerant quantum computation with nondeterministic entangling gates, Phys. Rev. A **97**, 030301 (R) (2018).
[13] M. Pant, D. Towsley, D. Englund, and S. Guha, Percolation thresholds for photonic quantum computing, Nat. Commun. **10**, 1070 (2019).
[14] H. Weinfurter, Experimental Bell-state analysis, Europhys. Lett. **25**, 559 (1994).
[15] J. Calsamiglia and N. Lütkenhaus, Maximum efficiency of a linear-optical Bell-state analyzer, Appl. Phys. B **72**, 67 (2001).
[16] S. Bartolucci, P. Birchall, H. Bombín, H. Cable, C. Dawson, M. Gimeno-Segovia, E. Johnston, K. Kieling, N. Nickerson, M. Pant, F. Pastawski, T. Rudolph, and C. Sparrow, Fusion-based quantum computation, Nat. Commun. **14**, 912 (2023).
[17] K. Sahay, J. Claes, and S. Puri, Tailoring fusion-based error correction for high thresholds to biased fusion failures, Phys. Rev. Lett. **131**, 120604 (2023).

[18] S. Paesani and B. J. Brown, High-threshold quantum computing by fusing one-dimensional cluster states, Phys. Rev. Lett. **131**, 120603 (2023).
[19] W. P. Grice, Arbitrarily complete Bell-state measurement using only linear optical elements, Phys. Rev. A **84**, 042331 (2011).
[20] P. W. Shor, Scheme for reducing decoherence in quantum computer memory, Phys. Rev. A **52**, R2493 (1995).
[21] T. C. Ralph, A. J. F. Hayes, and A. Gilchrist, Loss-tolerant optical qubits, Phys. Rev. Lett. **95**, 100501 (2005).
[22] F. Ewert, M. Bergmann, and P. van Loock, Ultrafast long-distance quantum communication with static linear optics, Phys. Rev. Lett. **117**, 210501 (2016).
[23] S.-W. Lee, T. C. Ralph, and H. Jeong, Fundamental building block for all-optical scalable quantum networks, Phys. Rev. A **100**, 052303 (2019).
[24] T. J. Bell, L. A. Pettersson, and S. Paesani, Optimizing graph codes for measurement-based loss tolerance, PRX Quantum **4**, 2 (2023).
[25] See Supplemental Material at http://link.aps.org/supplemental/10.1103/PhysRevLett.133.050605 for details of the encoded-fusion scheme with linear optics, encoded-fusion networks, and encoded resource states, which includes Refs. [26–29].
[26] H. Bombín, I. H. Kim, D. Litinski, N. Nickerson, M. Pant, F. Pastawski, S. Roberts, and T. Rudolph, Interleaving: Modular architectures for fault-tolerant photonic quantum computing, arXiv:2103.08612.
[27] H. Bombin, C. Dawson, N. Nickerson, M. Pant, and J. Sullivan, Increasing error tolerance in quantum computers with dynamic bias arrangement, arXiv:2303.16122.
[28] M. Varnava, D. E. Browne, and T. Rudolph, How good must single photon sources and detectors be for efficient linear optical quantum computation?, Phys. Rev. Lett. **100**, 060502 (2008).
[29] S. H. Lee and H. Jeong, Graph-theoretical optimization of fusion-based graph state generation, Quantum **7**, 1212 (2023).
[30] F. Ewert and P. van Loock, 3/4-efficient Bell measurement with passive linear optics and unentangled ancillae, Phys. Rev. Lett. **113**, 140403 (2014).
[31] H. A. Zaidi and P. van Loock, Beating the one-half limit of ancilla-free linear optics Bell measurements, Phys. Rev. Lett. **110**, 260501 (2013).
[32] S.-W. Lee, K. Park, T. C. Ralph, and H. Jeong, Nearly deterministic Bell measurement for multiphoton qubits and its application to quantum information processing, Phys. Rev. Lett. **114**, 113603 (2015).
[33] S.-W. Lee, K. Park, T. C. Ralph, and H. Jeong, Nearly deterministic Bell measurement with multiphoton entanglement for efficient quantum-information processing, Phys. Rev. A **92**, 052324 (2015).
[34] A. Bolt, G. Duclos-Cianci, D. Poulin, and T. M. Stace, Foliated quantum error-correcting codes, Phys. Rev. Lett. **117**, 070501 (2016).
[35] J. P. Bonilla Ataides, D. K. Tuckett, S. D. Bartlett, S. T. Flammia, and B. J. Brown, The XZZX surface code, Nat. Commun. **12**, 2172 (2021).
[36] J. Claes, J. E. Bourassa, and S. Puri, Tailored cluster states with high threshold under biased noise, npj Quantum Inf. **9**, 9 (2023).
[37] M. B. Hastings and J. Haah, Dynamically generated logical qubits, Quantum **5**, 564 (2021).
[38] M. Davydova, N. Tantivasadakarn, and S. Balasubramanian, Floquet codes without parent subsystem codes, PRX Quantum **4**, 020341 (2023).
[39] I. Schwartz, D. Cogan, E. R. Schmidgall, Y. Don, L. Gantz, O. Kenneth, N. H. Lindner, and D. Gershoni, Deterministic generation of a cluster state of entangled photons, Science **354**, 434 (2016).
[40] D. Istrati, Y. Pilnyak, J. Loredo, C. Antón, N. Somaschi, P. Hilaire, H. Ollivier, M. Esmann, L. Cohen, L. Vidro, C. Millet, A. Lemaître, I. Sagnes, A. Harouri, L. Lanco, P. Senellart, and H. S. Eisenberg, Sequential generation of linear cluster states from a single photon emitter, Nat. Commun. **11**, 5501 (2020).
[41] R. Uppu, L. Midolo, X. Zhou, J. Carolan, and P. Lodahl, Quantum-dot-based deterministic photon-emitter interfaces for scalable photonic quantum technology, Nat. Nanotechnol. **16**, 1308 (2021).
[42] C.-Y Lu and J.-W. Pan, Quantum-dot single-photon sources for the quantum internet, Nat. Nanotechnol. **16**, 1294 (2021).
[43] S. Bartolucci, P. M. Birchall, M. Gimeno-Segovia, E. Johnston, K. Kieling, M. Pant, T. Rudolph, J. Smith, C. Sparrow, and M. D. Vidrighin, Creation of entangled photonic states using linear optics, arXiv:2106.13825.
[44] B. Li, S. E. Economou, and E. Barnes, Photonic resource state generation from a minimal number of quantum emitters, npj Quantum Inf. **8**, 11 (2022).
[45] P. Thomas, L. Ruscio, O. Morin, and G. Rempe, Efficient generation of entangled multiphoton graph states from a single atom, Nature (London) **608**, 677 (2022).
[46] D. Cogan, Z.-E. Su, O. Kenneth, and D. Gershoni, Deterministic generation of indistinguishable photons in a cluster state, Nat. Photonics **17**, 324 (2023).
[47] S. H. Lee, S. Omkar, Y. S. Teo, and H. Jeong, Parity-encoding-based quantum computing with Bayesian error tracking, npj Quantum Inf. **9**, 39 (2023).
[48] B. Pankovich *et al.*, preceding Letter, High-photon-loss threshold quantum computing using GHZ-state measurements, Phys. Rev. Lett. **133**, 050604 (2024).
[49] R. Prevedel, P. Walther, F. Tiefenbacher, P. Böhi, R. Kaltenbaek, T. Jennewein, and A. Zeilinger, High-speed linear optics quantum computing using active feed-forward, Nature (London) **445**, 65 (2007).
[50] S. Bartolucci, P. Birchall, D. Bonneau, H. Cable, M. Gimeno-Segovia, K. Kieling, N. Nickerson, T. Rudolph, and C. Sparrow, Switch networks for photonic fusion-based quantum computing, arXiv:2109.13760.
[51] H. Bombín, C. Dawson, R. V. Mishmash, N. Nickerson, F. Pastawski, and S. Roberts, Logical blocks for fault-tolerant topological quantum computation, PRX Quantum **4**, 020303 (2023).